IEEE/CSC & ESAS SUPERCONDUCTIVITY NEWS FORUM (global edition), January 2016.
EUCAS 2015 preprint 3A-LS-P-07.09. Submitted to *IEEE Trans. Appl. Supercond.* for possible publication.

Dynamics of rotating Superconducting Magnetic Bearings in Ring Spinning

M. Sparing, A. Berger, F. Wall, V. Lux, S. Hameister, D. Berger, M. Hossain, A. Abdkader, G. Fuchs, C. Cherif, L. Schultz

***Abstract* — A superconducting magnetic bearing (SMB) consisting of a stationary superconductor in a ring-shaped flow-through cryostat and a rotating permeant magnetic (PM) ring is investigated as potential twist element in the textile technological process of ring spinning. Since the dynamic behavior of the rotating PM influences the yarn as well as the stability of spinning process, these factors are studied in this paper considering the acting forces of the yarn on the PM-ring, its vibration modes and the resulting oscillation amplitudes.**

For the assessment of a safe field cooling distance during the operation of the rotating SMB in a rings spinning machine, a correct calculation of the resonance magnification is particularly important. Therefore, the decay constant δ of the damped oscillation was measured as a function of the field cooling distance (FCD) and the displacement. The observed increase of the decay constant δ with the initial lateral displacement and decreasing FCD is discussed in correlation to the number of depinned flux lines.

***Index Terms*— levitation, superconducting magnetic bearing, spinning, textile technology, Yttrium barium copper oxide**

I. Introduction

Rotating machines, e.g. motor and flywheels are highly investigated potential applications for rotating superconducting magnetic bearings (SMB) [1]-[3]. The prospect of a passive bearing and contact free rotation is especially attractive for devices, were frictional wear and heat are the limiting factor for the productivity. This is also the case in the textile technological process of ring spinning, were SMBs are recently being investigated as novel twist elements [4]. In this paper, we discuss the specific challenges arising from the integration of an SMB as twist element in a ring spinning machine.

Ring spinning is currently the most commonly used technology for the production of short staple yarn. The primary productivity-limiting factor of this process is frictional heat in the twist element, which consist of a c-shaped clip (the traveler) dragged along a ring-rail by the yarn during spinning and winding. This procedure twists the fibers thereby form sand strengthens the yarn. Details of the spinning process and various concepts to improve or replace the ring-traveler system are described in the literature [5], [6]. The replacement of the ring-traveler system by an SMB eliminates the problem of frictional heat in the existing system. A detailed description of this process can be found in references [7]-[9].

Manuscript received XX, 2015.

This work is funded by the German Research Foundation, DFG (Project Nr. CH 174/33-1).

M. Sparing, D. Berger, A. Berger, F. Wall, G. Fuchs and L. Schultz are with the IFW Dresden, Institute for Metallic Materials, P.O. Box 270116, D-01171 Dresden, Germany (e-mail: m.sparing@ifw-dresden.de, phone: +493514659847).

M. Hossain, A. Abdkader and C. Cherif are with the Institute of Textile Machinery and High Performance Material Technology, Technical University of Dresden, 01062 Dresden, Germany

II. Ring spinning with an SMB twist element

A. The SMB twist element

The ring-traveler system is replaced by a SMB twist element consisting of a superconducting ring in a closed flow-through cryostat and a permanent magnetic ring (PM-ring) encased in a steel shell (see Fig. 1). The eyelet for the yarn is integrated in the steel. In our system the superconducting material is an assembled YBCO-ring (outer Ø = 80 mm) and the PM-ring is a matching sintered NdFeB ring, which is similar to that system described in reference [8] and [10]. Each rotation of the yarn driven PM-ring imparts the required twist in the yarn during spinning. We recently demonstrated the spinning of good quality yarn with the presented SMB twist element at rotational speeds up to 15 000 rpm [9].

The SMB twist element has the potential to spin yarn at much higher speed compared to the existing ring-traveler system. The development of a novel ring spinning machine with SMB, aiming at a target rotation speed of up to 50 000 rpm, require a better understanding of the behavior of SMBs under application conditions. Because the static and dynamic behavior of the rotating PM-ring influence the yarn tension as well as the stability of spinning process, the dynamics of the rotating PM-ring are investigated in this paper considering the acting forces of the yarn on the PM-ring, its vibration modes and the resulting oscillation amplitudes.

B. Mathematical model of the SMB twist element

The SMB as twist element in the ring spinning machine is mathematically described as a spring-mass-damper system, which is excited by an external force, i.e. the yarn force (Fig. 1). The yarn force acts at the eccentric contact point between yarn and permanent magnet (PM), i.e. the eyelet at the inner bore of the steel shell around the PM-ring.

The yarn force F_G, can be separated into two in-plain components $F_G{}^z$ (axial) und $F_G{}^r$ (radial) and the circumferential component $F_G{}^\phi$. The yarn forces $F_G{}^z$ and $F_G{}^r$ aim at displacing the PM-ring in radial, axial and tilt direction.

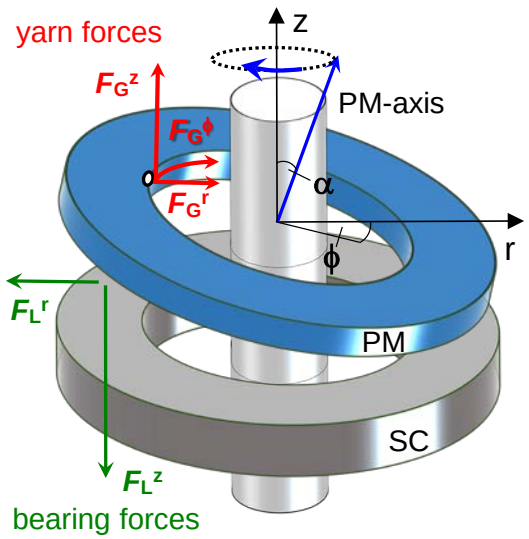

Figure 1: The SMB is subjected to an external yarn force F_G, applying at the eccentric contact point between yarn and permanent magnet (PM). The directional components of F_G are responsible for the displacement and the rotation of the PM ring. The restoring forces of the bearing F_L^z in axial and F_L^r in radial direction countervail this displacement.

They are counteracted by the restoring forces of the bearing F_L^z in axial and F_L^r in radial direction. The bearing stiffness $k_i = dF_i/dx_i$ (index i being the displacement direction) causes forced oscillations in both directions. There is no restoring force in circumferential direction for this round SMB geometry, thus F_G^ϕ acts as driving force for the free rotation of the PM-ring.

The rotation of the PM-ring is superimposed by the above mentioned forced oscillations. This rotation speed dependent oscillation of the PM-ring can be separated into three modes, which are expressed by the equations (1) - (3).

$$r'' + 2\delta_r\, r' + \omega_{d,r}{}^2\, r = F^r(t)/m_{PM} \quad (1)$$

$$z'' + 2\delta_z\, z' + \omega_{d,z}{}^2 z = F^z(t)/m_{PM} \quad (2)$$

$$\alpha'' + 2\delta_\alpha\, \alpha' + \omega_{d,\alpha}{}^2\, \alpha = F_G{}^z\,(t)\, R_i / J_\alpha \quad (3)$$

Eqs. (1) and (2) describe the lateral and vertical oscillation of the PM-ring, approximated as mass point, around its center of mass. With m_{PM} as mass of the PM ring, δ as decay constant of the damped oscillation without external force and $F^i(t) = F_G{}^i \cos(\omega t)$. For the tilt oscillation (Eq. 3) the PM ring is considered as rigid body, with α as tilt angle, J_α as the moment of inertia and $\omega_{d,i}$ as resonance frequency.

The amplitude of the oscillation $A(\omega)$ is described by the expression

$$A(\omega) = \frac{F_G}{m_{PM}} \frac{1}{\sqrt{\left(\omega^2 - \omega_0^2\right)^2 + 4\delta^2\omega^2}} \quad (4)$$

with ω and $\omega_0 = (k_i/m)^{0.5}$ as the angular frequency and the Eigen angular frequency of the system, respectively.

While the stationary stiffness k_i of SMBs is easily accessible by force vs. displacement measurements, the determination of the decay constant and the dynamic stiffness is more complex, which makes a correct prediction of maximum amplitude during operation difficult. So far, the resonance magnification, $A(\omega_0)/A(0) \approx \omega_0 / 2\delta$ in our SMB system, could only be estimated by using stationary values for the stiffness, whereas the decay constant had to be taken from literature values for axial vibrations [8], [11], [12]. As a result, the SMB was operated in the ring spinning machine with FCD = 5 mm, i.e. 2 mm above the cryostat, in order to prevent a contact between cryostat and rotating PM-ring at the resonance frequency. A more precise $A(\omega)$ estimated from a decay constant measured in our actual SMB system and the additional measurement of $A(\omega)$ during operation would allow to design SMB twist elements with smaller FCDs and hence enable an increased stiffness and stability of the bearing.

III. Measurement of the Decay Constant

A. Experimental setup

The measurement setup in figure 2 consists of a superconducting YBCO-ring (outer Ø = 80 mm, inner Ø = 50 mm), cooled to 77 K in flow-through cryostat, and the matching NdFeB-ring, above the cryostat.

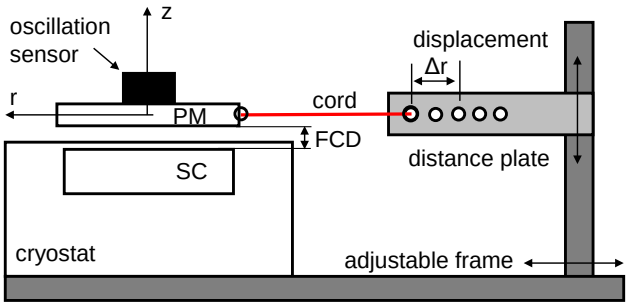

Figure 2: Setup for the measurement of the damped oscillation for a lateral displacement. The initial position without displacement, during field cooling is shown.

The permeant magnetic ring (PM-ring) is placed in a fixed field cooling distance (FCD) to the surface of the superconductor (SC). The PM-ring is encased in a shell with a small eyelet to which a cord with low elasticity is connected. The other end of the cord is knotted to a washer (small ring). After field cooling the SMB, the initial displacement Δr of the PM-ring is realized by fixing the washer to a bolt in one of the holes in the distance plate. When the bolt is pulled, the damped oscillation of the PM-ring back into its equilibrium position is measured with a Brüel&Kjaer 3-axis acceleration sensor. The parallel measurement of the acceleration in three orthogonal directions ensures that the direction of the measured signal and the initial displacement direction are the same.

The initial displacement in axial direction Δz can be measured in a similar fashion with a modification of the measurement setup shown in figure 2.

B. *Data analysis*

The measured damped oscillation of the PM-ring in the initial displacement direction roughly follows an exponential decay of a damped sine wave function [11]. The time-dependent acceleration $a(t)$ is given by

$$a(t) = a_0 + \mathrm{A} * e^{-\delta t} \sin\left(\frac{2\pi\,(t\text{-}t_c)}{T_d}\right) \qquad (5)$$

The acceleration a and the time t are the measured values, whereas the decay constant δ and the time period of the oscillation T_d are fitting parameters. The characteristic angular frequency of the damped oscillation is $\omega_D = 2\pi/T_d$.

Figure 3 shows the acceleration vs. time measurement for a field cooling distance (FCD) of 5 mm after an initial displacement of the PM-ring of Δr = 5.4 mm. The measured data can only be fitted by Eq. (5) using different decay constants for two different time intervals. The decay constant delta δ can also be determined from the maxima of $a(t)$ according to

$$a_{max}(t) = \mathrm{A} * e^{-\delta t} \qquad (6)$$

The decrease of the decay constant δ in the decay curves (Eq. 6) indicates that the decay of the damped oscillation in radial direction is not constant over a longer time period. A similar observation was reported by Futamura *et al*. [12] and Sakei *et al*. [13] in an SMB for initial displacements in axial direction.

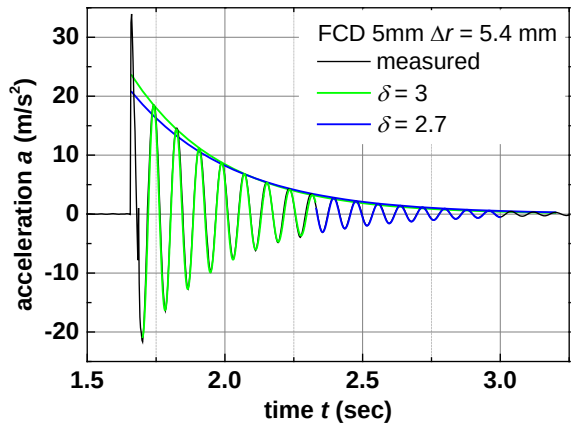

Figure 3: Damped oscillation of the PM-ring for a field cooling distance FCD = 5 mm after an initial radial displacement of Δr = 5.4 mm. The decay constant δ changes during the course of the oscillation.

C. *Dependency of the decay constant on initial displacement*

It is not obvious, whether the observed damping behavior of the SMB over time is driven by external factors (e.g. air friction) or if the decay constant varies as a function of the initial or even the effective displacement. Therefore the damped oscillation of the PM-ring was measured for a number of initial displacements Δr at two different field cooling distances (FCD = 5 mm and 6 mm). Each measured $a(t)$ is fitted by Eq. (5) in the time interval from the first minimum to approx. the tenth maximum of the respective function. The resulting decay constants δ and time periods T_d are shown in figure 4 (a) and (b). The values for the initial displacement Δr were taken from the double integrated a(t) measurements at the time of the second maximum of a(t), which corresponds to the first minimum of the displacement.

Generally, the observed decay constant for SMBs is small owing to the low external friction in the system due to air friction and dissipation in the YBCO ring. For both FCDs we observe an increase of δ with the initial lateral displacement which can be understood by assuming that the pinned flux lines are depinned, when the PM ring is moved from its initial position at Δr = 0 to Δr. As depinning of flux lines causes dissipation, the damping in the SMB increases with the average number of pinning centres within the displacement Δr. Hence, an almost linear increase of the decay constant with Δr is expected.

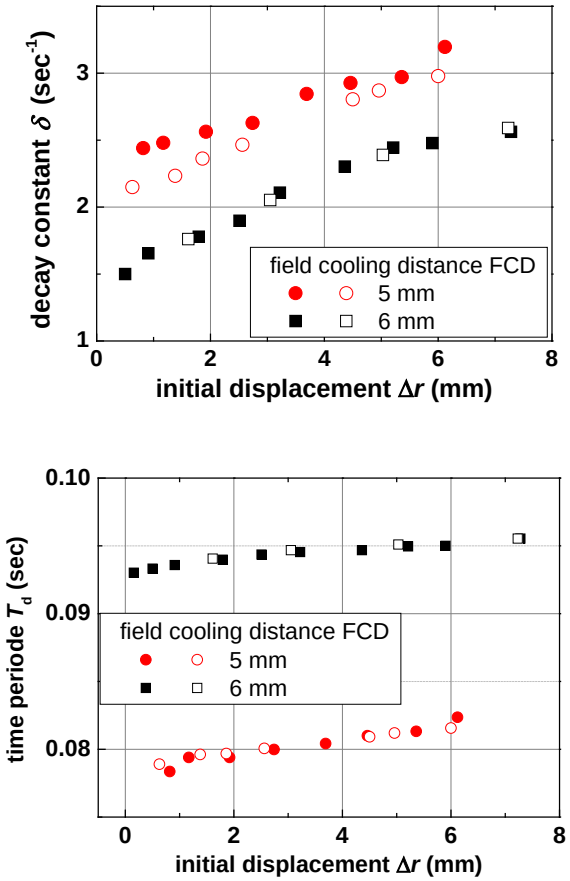

Figure 4: (a) Decay constant δ and (b) time period T_d versus initial lateral displacement Δr for field cooling distance FCD = 5 mm and 6 mm. The open symbols represent a repetition of the experiment and give an indication for the accuracy of measurement setup.

In Fig. 4 (b), only a slight increase of the time period with the initial lateral displacement is observed for both FCDs. This means that the resonance frequency $\omega_D = 2\pi/T_d$ and the dynamic stiffness $k_d = m\,\omega_0^2$ which are closely related to T_d, slightly decrease with the initial displacement.

At the smaller field cooling distance, a higher field is trapped within the superconductor. Due to the larger number of pinned flux lines, the damping becomes stronger (see Fig. 4 a) and the stiffness of the SMB enhances which gives rise to an increase of the resonance frequency and a lower time period (see Fig. 4 b). Thereby, the resonance frequency is much more influenced by the field cooling distance than by the initial displacement as shown in Fig. 4 (b).

IV. Calculation of the Oscillation Amplitude

The dependence of the decay constant δ of the initial displacement has consequences for the rotation frequency dependent amplitude of the oscillation $A(\omega)$ during the rotation of the PM-ring. The amplitude $A(\omega)$ increases with decreasing δ (see Eq. 4), which is most noticeable at the resonance frequency and best illustrated by the resonance magnification $A(\omega_0)/A(0) \approx \omega_0 / 2\delta$, for small damping with $\omega_0 \approx \omega_D$.

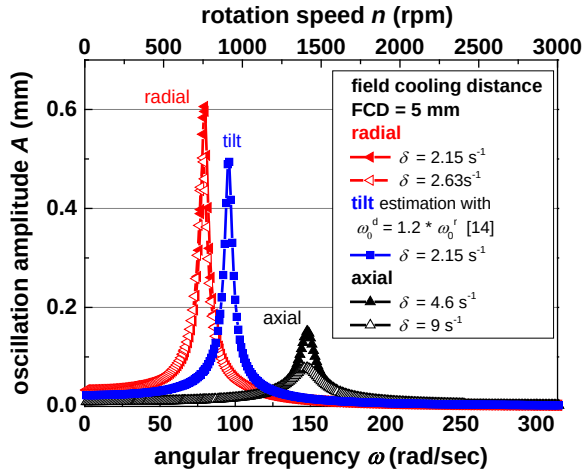

Figure 5: Oscillation amplitude $A(\omega)$ of the PM-ring with $\delta = f(\Delta r)$.

Figure shows the calculated amplitude of the oscillations in lateral, tilt and axial direction during rotation of the PM-ring [8]. The yarn force F_G and the mass m_{PM} = 241 g are measured values from the ring spinning process [9] with an SMB, whereas ω_0 and δ are determined from the acceleration vs. initial displacement measurement described above. The yarn force F_G = 0,05 N remains constant for n < 3400 rpm, whereas between n = 5000 rpm and 25 000 rpm the yarn force follows a polynomic function $F_G = 10^{-9}*(10582{,}4\ n + 1{,}22607\ n^2)$ [9]. Although F_G was measured as the total force acting on the yarn in the ring spinning system with SMB, the directional components of F_G are still unknown. Therefore all calculations assume that the maximum yarn force $F_G(\omega)$ acts in each direction. This leads to an overestimation of the absolute $A(\omega)$ and gives us a safety factor for the system design. The stiffness and damping for the tilt mode could not be measured yet, and were estimated from $\omega_0{}^t = 1.2\ \omega_0{}^r$ [14].

The measured damped resonance frequency $\omega_D = (\omega_0^2 - \delta^2)^{0.5}$ where the amplitude of the oscillation $A(\omega)$ is maximal remains below 1500 rpm for all modes. These small rotational speeds are not relevant for the actual spinning process, which takes place between 5000 and 25 0000 rpm. However, during the acceleration and deceleration of the process, these frequencies occur and the respective oscillation amplitudes have to be considered for the setup and operation of the SMB system in the ring-spinning machine.

In figure 5, $A(\omega)$ is shown for the radial, axial and tilt mode with two different decay constants, one measured for a small and the other measured for a larger initial displacement Δr (values taken from figure 4 a). As explained above, $A(\omega_D)$ increases with decreasing δ, i.e. with smaller initial displacements Δr. Hence, the amplitude may be underestimated, if the decay constant measured for a high initial displacement is used (open symbols in Fig. 5), e.g. the resonance magnification for FCD = 5 mm rises from 12 to 18 between Δr = 6.1 mm and 0.6 mm.

Which decay constant has to be used in order to calculate $A(\omega_D)$ correctly is not known so far. This has to be verified in the future by a direct measurement of the oscillation amplitude of the SMB in the ring spinning machine.

V. Summary

The correct prediction of the resonance amplitude $A(\omega_D)$ is crucial for the assessment of a safe field cooling distance for the operation of an SMB as twist element in the ring spinning machine. The calculation of the oscillation amplitude $A(\omega)$ requires the knowledge of acting forces as well as the decay constant δ of the damped oscillation. A simple measurement setup is described, with which δ can be determined for lateral and vertical displacement of the PM-ring. The decay constant δ is shown to depend strongly on the initial radial displacement Δr and the field cooling distance FCD. Since the damping in the SMB is caused by the depinning of flux lines during oscillation, the linear increase of δ with Δr can be attributed to an increases of the average number of pinning centres within the displacement.

References

[1] J. R. Hull, "Superconducting bearings," *Superconductor science & technology*, vol.13, no. 2, pp. R1–R15, Feb. 2000.
[2] G. Krabbes, G. Fuchs, W. R. Canders, H. May and R. Palka , "High Temperature Superconductor Bulk Materials" Weinheim, Germany: WILEY-VCH , 2006
[3] F. N. Werfel, U. Floegel-Delor, R. Rothfeld, T. Riedel, B. Goebel, D. Wippich, and P. Schirrmeister, "Superconductor bearings, flywheels and transportation," *Superconductor Science & Technology*, vol. 25, no. 1, Article nr. 014007, Jan. 2012.
[4] C. Cherif, A. Abdkader, L. Schultz, D. Berger, O. de Haas, L. Kühn, "Spooling and spinner device of a ring spinning frame or a ring twisting frame, and ring spinning and ring twisting method, "Patent WO 2012/100964 A2, International, 2012.
[5] A. Marzoli, "Rotary Ring for Spinning and Twisting Ring machines," U.S. Patent 4, 161,863, 1979.
[6] F. Abdel-hady, Y. El Mogahzy, S. AbuElenin S and R. Abdel-Kader, "Innovative approach to high-speed spinning using a magnetically-elevated spinning ring," *AUTEX Res. J.* 2006; 6: 113–121.
[7] M. Hossain, A. Abdkader, C. Cherif, M. Sparing, D. Berger, G. Fuchs, and L. Schultz, "Innovative twisting mechanism based on superconducting technology in a ring-spinning system," *Textile Research Journal*, vol. 84, no. 8, pp. 871-880, May 2014.
[8] M. Sparing, M. Hossain, D. Berger, A. Berger, A. Abdkader, G. Fuchs, C. Cherif, L. Schultz, "Superconducting magnetic bearing as twist

element in textile machines," *IEEE Transactions on Applied Superconductivity* 25 (2015) Nr. 3, S. 3600504/1-4

[9] M. Hossain, A. Abdkader, C. Cherif, M. Sparing, A. Berger, D. Berger, G. Fuchs, and L. Schultz,, "Mathematical modelling and simulation of the dynamic yarn path using a superconducting magnet bearing in a ring spinning process," submitted for publication

[10] A. Berger, M. Hossain, M. Sparing, D. Berger, G. Fuchs, A. Abdkader, C. Cherif, and L. Schultz "Cryogenic system for a ring-shaped SMB and integration in a ring-spinning tester" *IEEE Trans. Appl. Supercond.* (submitted EUCAS 2015: 3A-LS-P-07.06)

[11] L. Kuehn, M. Mueller,, R. Schubert, C. Beyer, O. de Haas, and L. Schultz, "Static and dynamic behavior of a superconducting magnetic bearing using YBCO bulk material," *IEEE Transactions on Applied Superconductivity*, vol. 17, no. 2, part 2, pp. 2079-2082, Jun. 2007.

[12] M. Futamura, T. Maeda, H. Konishi, "Damping Characteristics of a Magnet Oscillating above a YBCO Superconductor," *Japanese Journal of Applied Physics* vol 37, pp 3961-3964 1998.

[13] I. Sakai and T. Higuchi, "Dynamic Properties of Magnetic Levitation System Using High-Temperature Superconductors," *IEEE Transactions on Applied Superconductivity*, vol. 21, no. 3, June 2011.

[14] A. Cansiz, J. R. Hull, and O. Gundogdu, "Translational and rotational dynamic analysis of a superconducting levitation system," *Superconductor Science & Technology*, vol. 18, no. 7, pp. 990-996, Jul. 2005.